PHYSICS OF COMPACT OBJECTS
AND THEIR BINARY INTERACTIONS

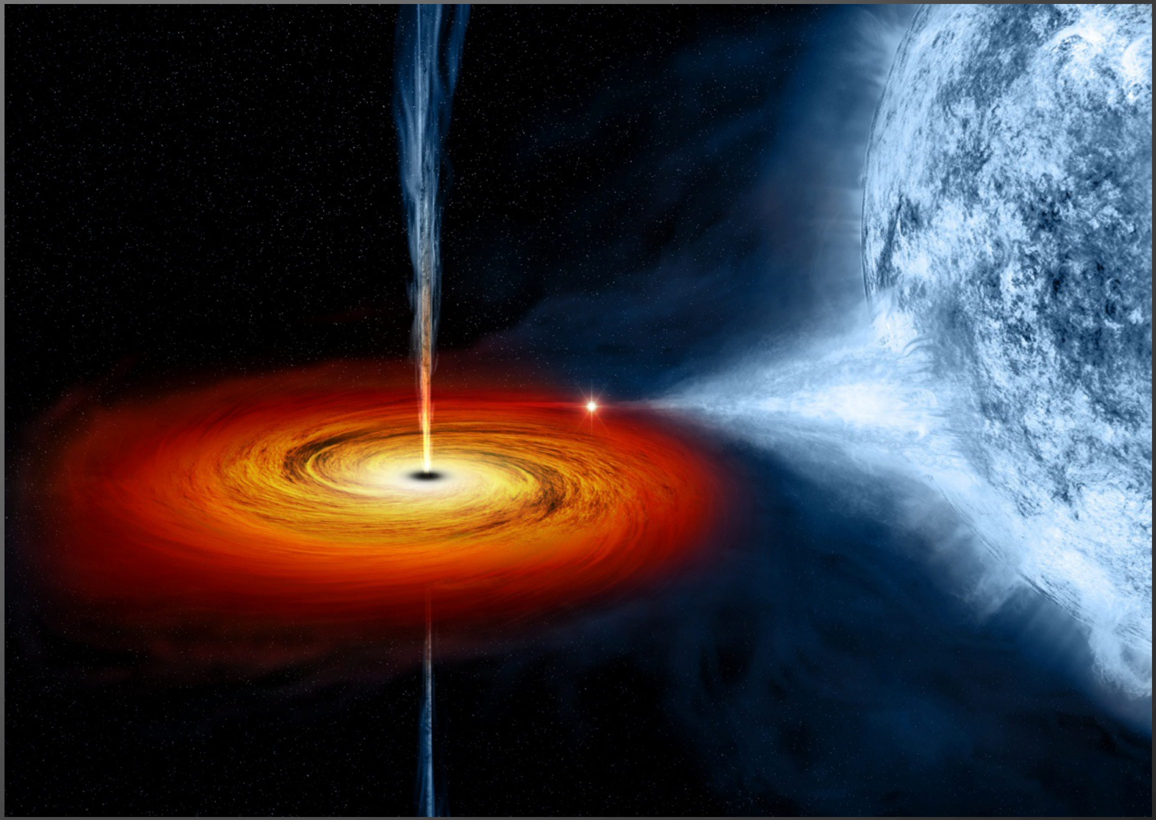

AALBORG UNIVERSITY

Thomas Tauris – Physics, Aalborg University

Structure of Neutron Stars

Cold equations-of-state above neutron drip

Last time

- EoS for $\rho_{drip} < \rho < \rho_{nuc}$
  - Baym-Bethe-Pethick (BBP) EoS
  - Stability of NSs
- EoS for $\rho > \rho_{nuc}$
  - Nucleon-nucleon interactions
  - Muons, hyperons, Δ-resonances, pion/kaon condensation
  - Superfluidity (glitches/cooling of NSs)
  - Bethe-Johnson (BJ) EoS
  - Quark (strange) stars / quark-novae
- Summary of EoS above neutron drip
- Structure of NSs
  - Cross section
  - Soft vs Stiff EoS
  - Observational constraints on M and R

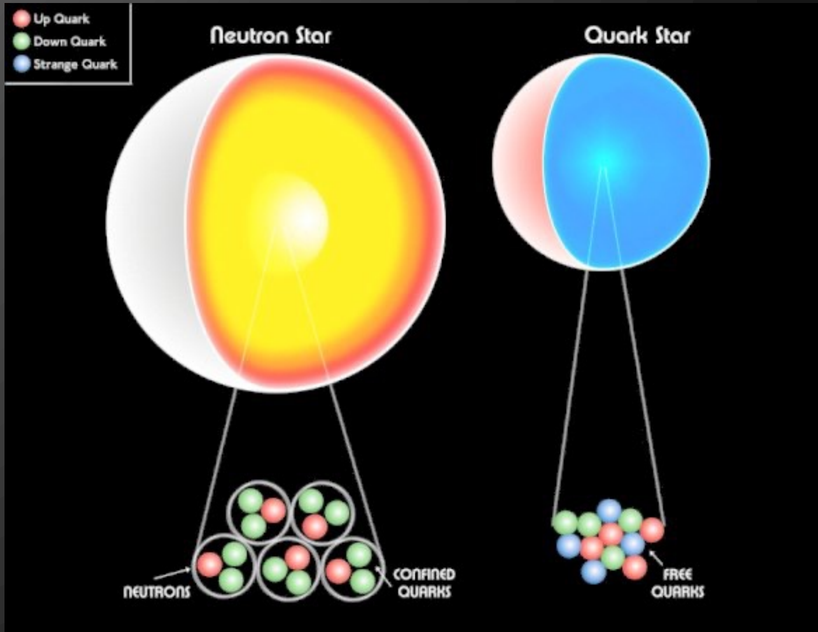

Programme

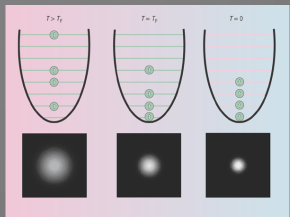

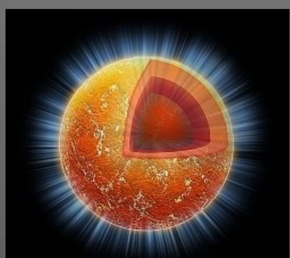

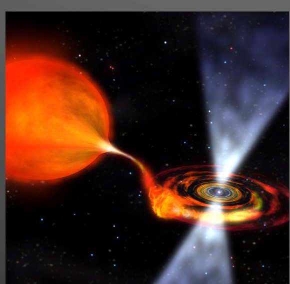

- **Introduction**
- **Degenerate Fermi Gases**
  Non-relativistic and extreme relativistic electron / (n,p,e^-) gases
- **White Dwarfs**
  Structure, cooling models, observations
- **Neutron Stars**
  Structure and equation-of-state
- **Radio Pulsars**
  Characteristics, spin evolution, magnetars, observations
- **Binary Evolution and Interactions**
  X-ray binaries, accretion, formation of millisecond pulsars, recycling
- **Black Holes**
  Observations, characteristics and spins
- **Gravitational Waves**
  Sources and detection, kilonovae
- **Exam**

Radio Pulsars

Characteristics, observations, spin evolution, magnetars

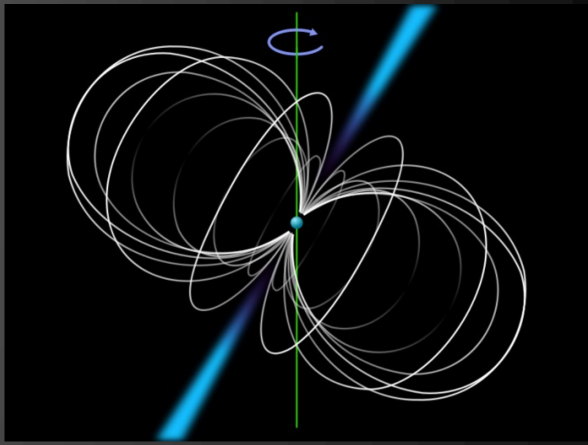

- Observational aspects of radio pulsars
  - The radio pulsar population in the Milky Way
  - Pulse profiles / Scintillation / Dispersion measure
  - Emission properties
- Spin evolution of pulsars in the $P\dot{P}$-diagram
  - The magnetic dipole model
  - Evolution with B-field decay
  - Evolution with gravitational wave emission
  - The braking index
  - True ages of radio pulsars
- Magnetars
  - Soft gamma-ray repeaters (SGRs) and Anomalous X-ray pulsars (AXPs)

Blackboard

Radio Pulsars

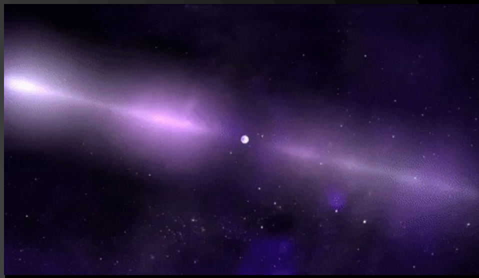

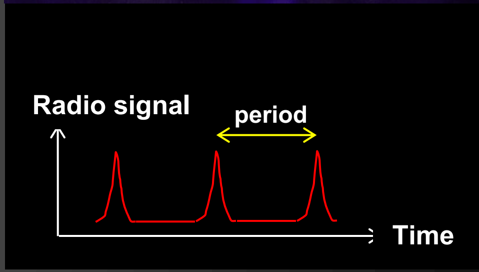

A pulsar is a perfect physics laboratory:

- ✓ ν = 700 Hz (P=1.4 ms – 23 sec.)
- ✓ B = 10^{13} G
- ✓ $\dot{E}_{rot} = 10^5\ L_\odot$ ($F = 10^{14}\ F_\odot$)
- ✓ M = 1.4 $M_\odot$
- ✓ R = 10 km

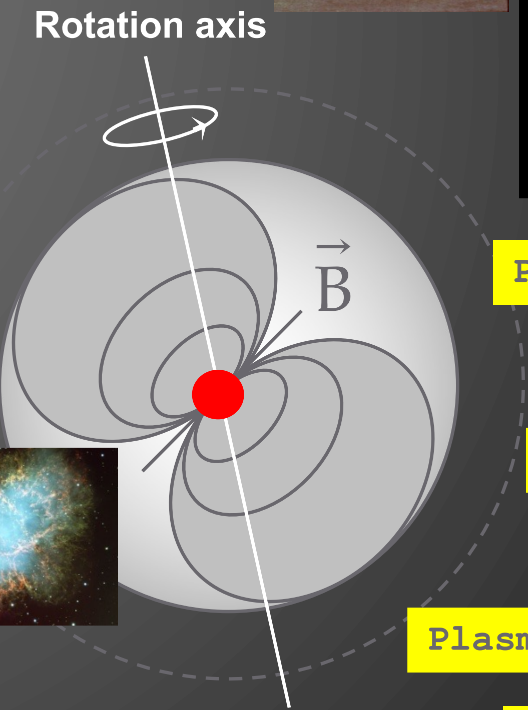

Giant atomic nucleus:

- ✓ A=10^{57} baryons, ρ_{core} = 2-10 $\rho_{nuclear}$

Magnetosphere:

- ✓ production of 10^{38} (e^-, e^+) per second
- ✓ TeV γ-rays
- ✓ e^- accelerated to 10^{16}eV, $\Delta\phi$ =10^{16} Volts

Particle physics

Nuclear physics

Solid state physics

Atom physics

Plasma physics

Relativity

a unique physics laboratory

Perfect clock:

- ✓ P = 0.001 557 806 448 872 75 seconds (PSR 1937+21)

Challenge atomic clocks

Radio Pulsar Emission

The surface intensity of the radio emission, I using a Planck function demonstrates that if the radio emission was caused by thermal black body radiation one would obtain an extremely high brightness temperature (leading to absurdly large particle energies) and therefore the radiation mechanism of a radio pulsar *must* be coherent (Most models invoke curvature radiation or a maser mechanism).

$$I_\nu = \frac{2h\nu^3}{c^2}\frac{1}{e^{h\nu/kT}-1} \qquad \left(I_\nu \propto \nu^{\alpha}\ ,\ \alpha = -1.5\right)$$

Planck function — Empirical evidence

$$Crab: \quad f = 0.48\ Jy \quad @\ 436\ MHz$$

$$(1\ Jansky = 10^{-23}\ erg\ cm^{-2}\ s^{-1}\ Hz^{-1}\ st^{-1})$$

$$\Rightarrow \quad kT \approx 10^{24}\ eV \quad (T \approx 10^{29}\ K)$$

Note: units for I_ν are equal to those for f (spectral radiance = flux density)

Ex.2

Detected radio pulsars in our Milky Way:

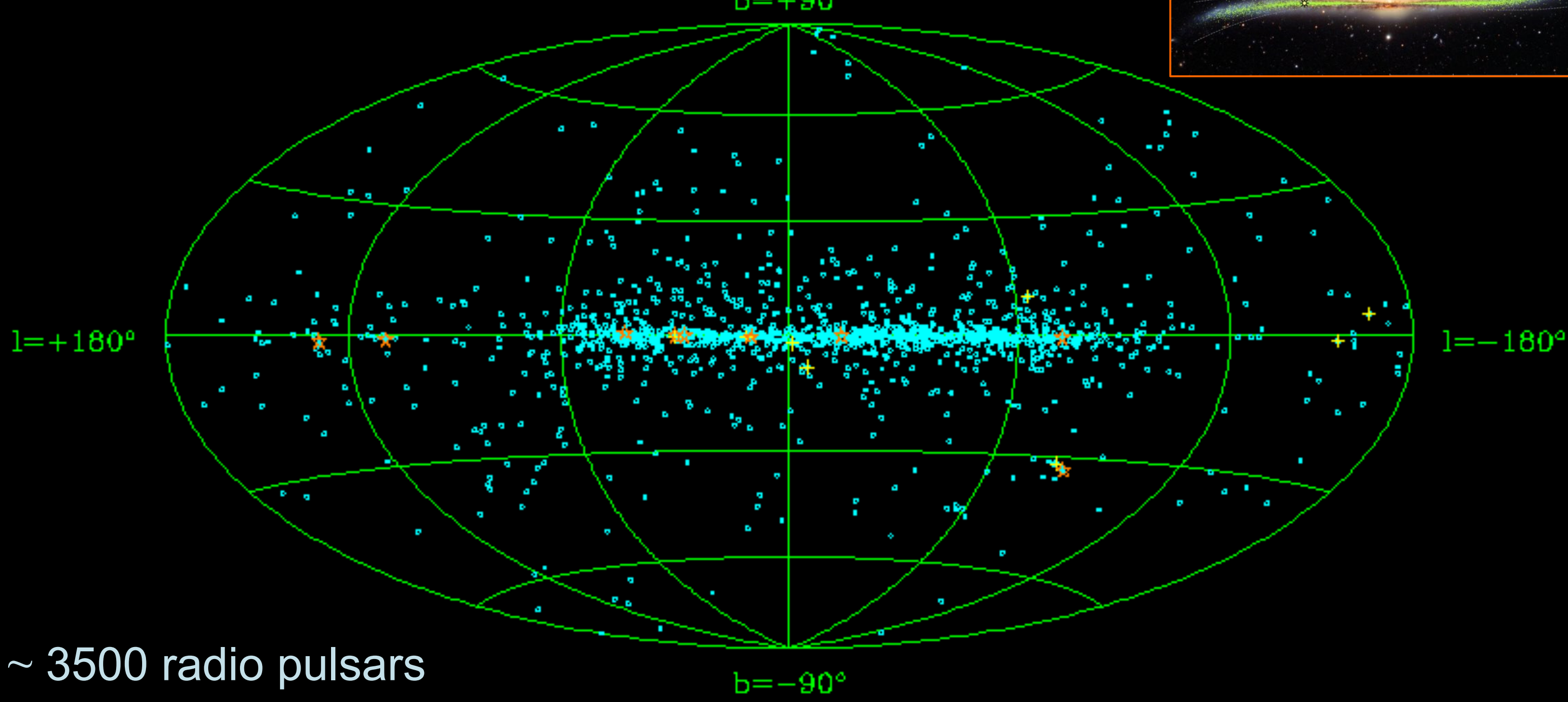

~ 3500 radio pulsars

~ 50 X-ray pulsars

~ 300 neutron stars in X-ray binary systems

- Pulsars are concentrated in the Galactic plane in star forming regions (OB star progenitors)
- Large spread is caused by high velocities (kicks imparted to NSs in supernova explosions)

Detected radio pulsars in our Milky Way:

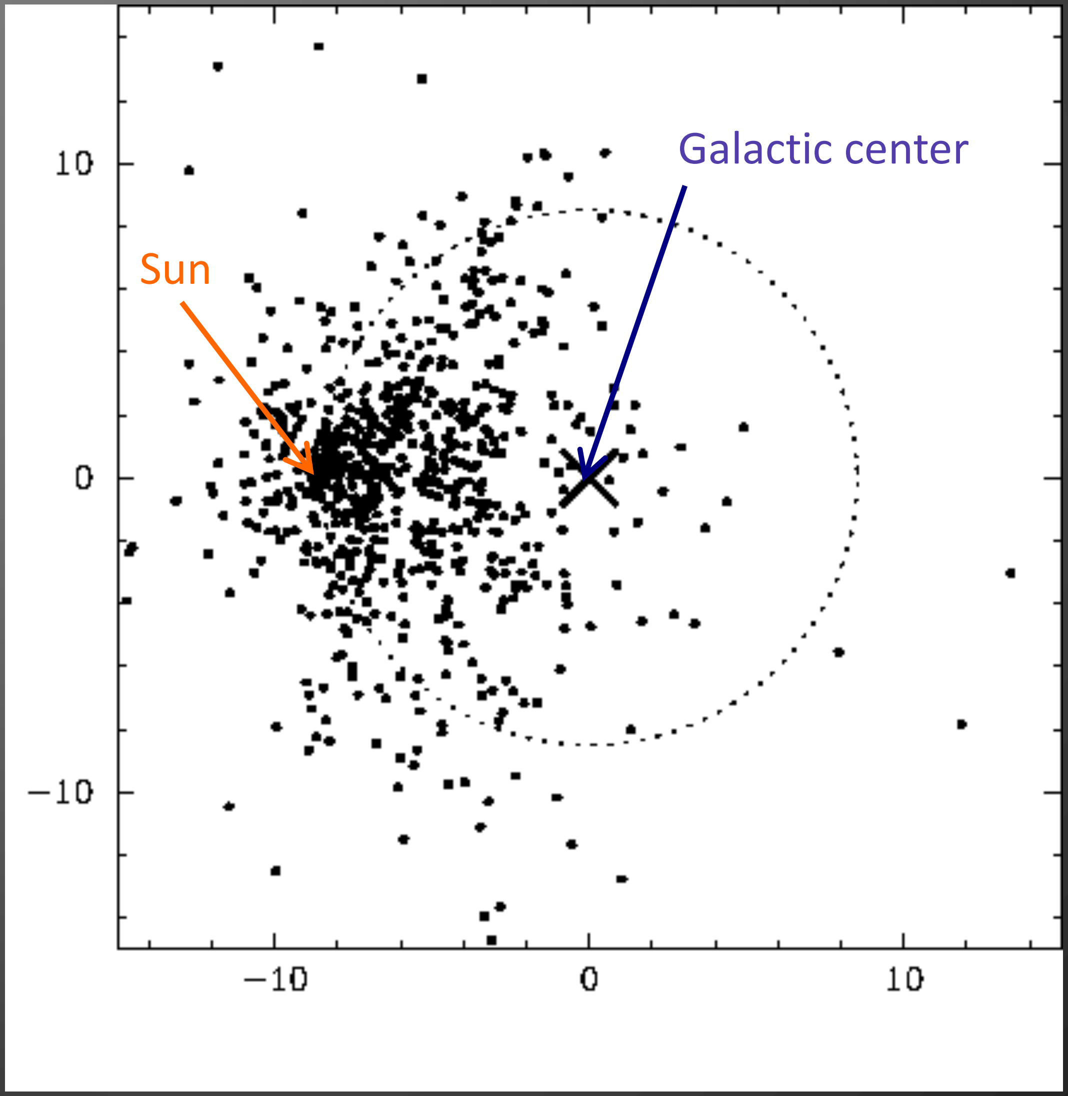

Discovery of radio pulsars with the SKA (Square-Kilometre Array)

Will increase number of known pulsars by a factor 5-10 (Keane et al. 2015)

Phase I @ 2024 – Phase II @ 2030? – Frequency range: 50 MHz to 14 GHz.

- SKA-low array (50 – 350 MHz) (dipole antennas)
- SKA-mid array (350 MHz – 14 GHz) (15 m. dish antennas)
- SKA-survey array (350 MHz – 4 GHz) (a compact array of parabolic dishes)

Pulsar pulse profiles

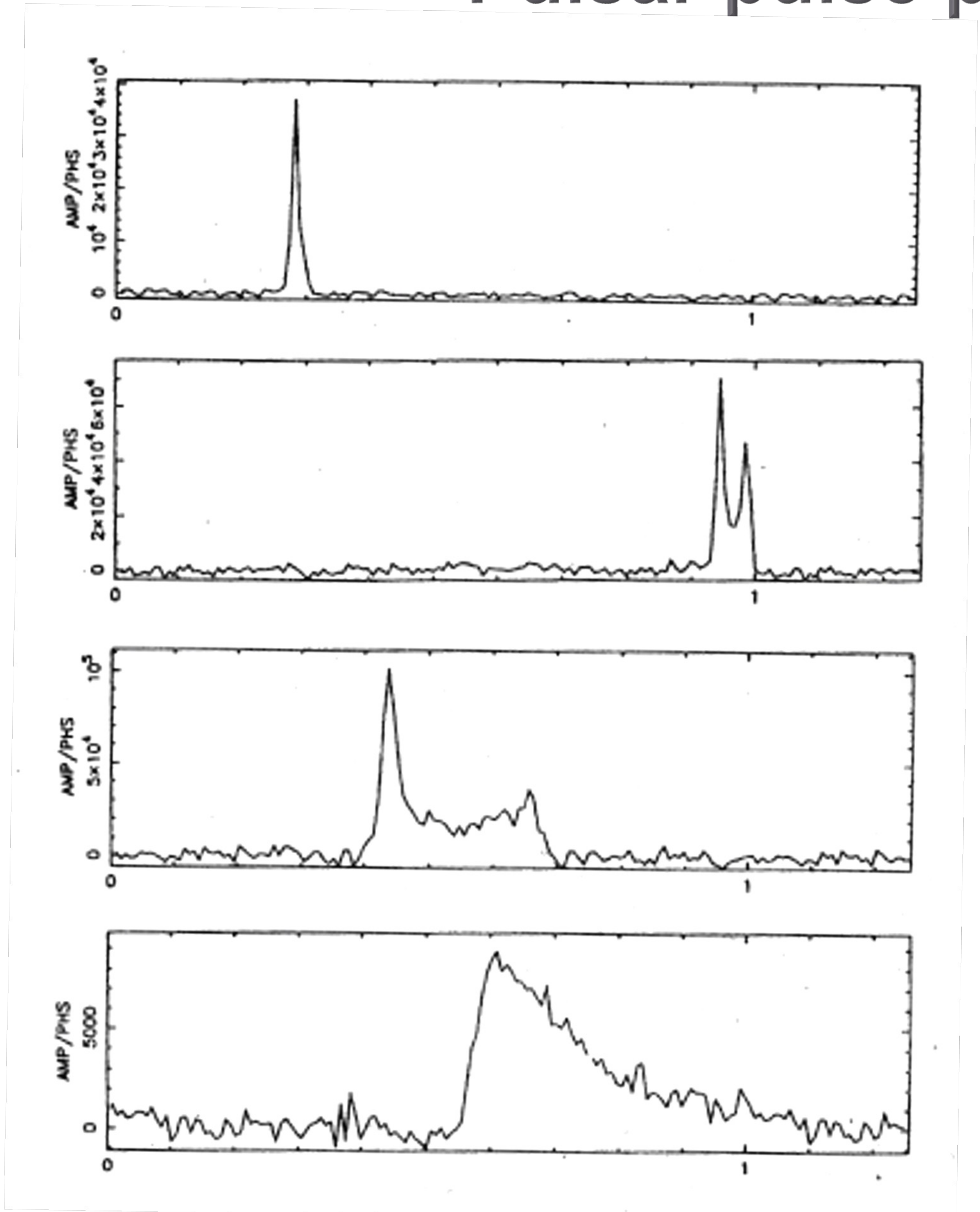

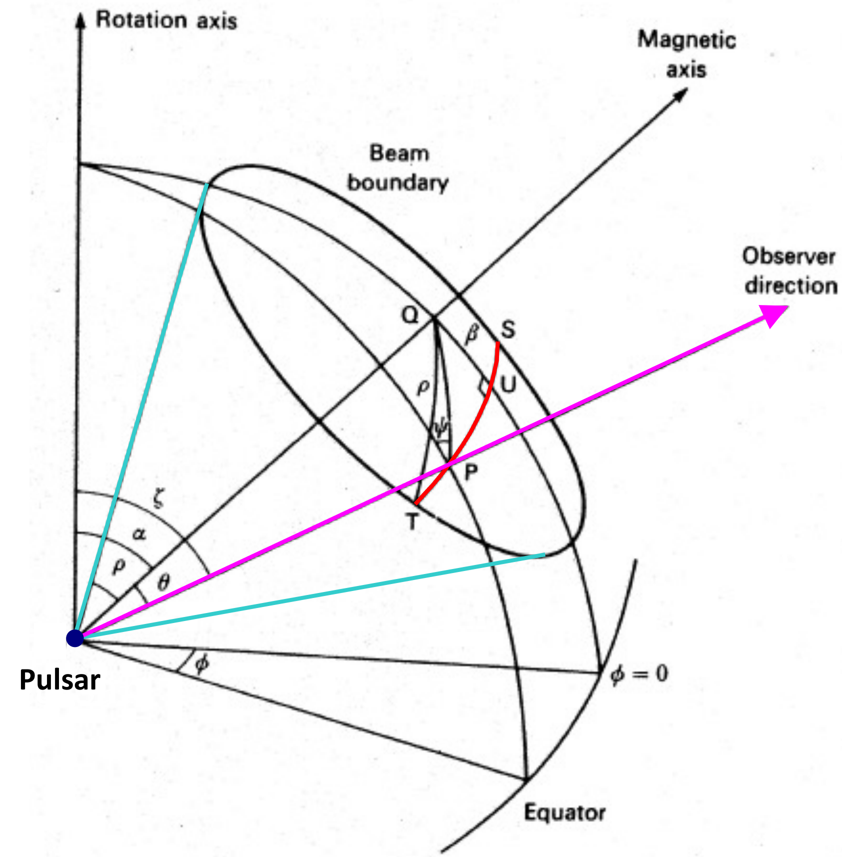

Pulsar pulse profiles

436, 660, 1420 MHz

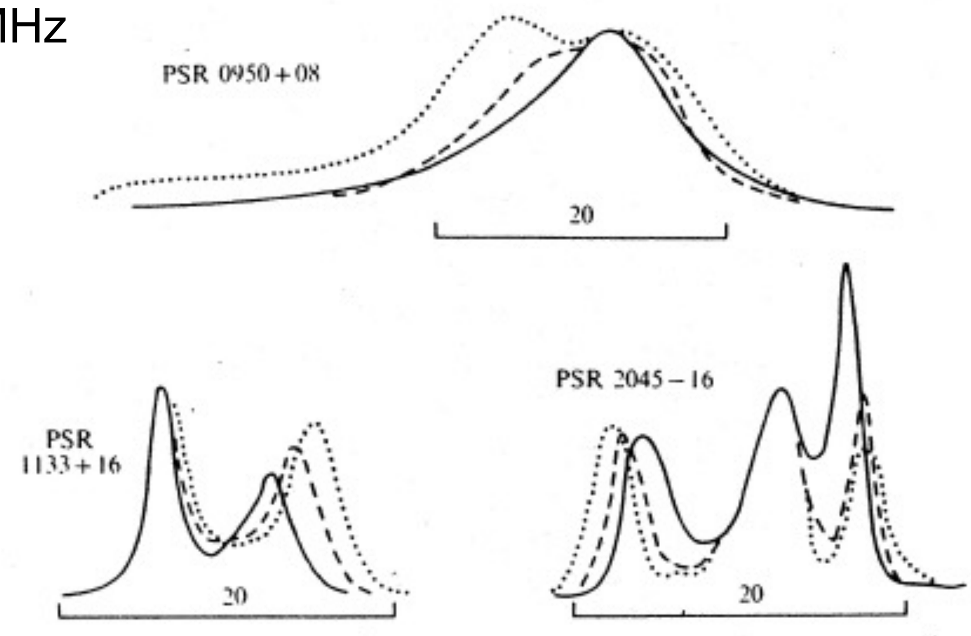

Pulsar pulse profiles

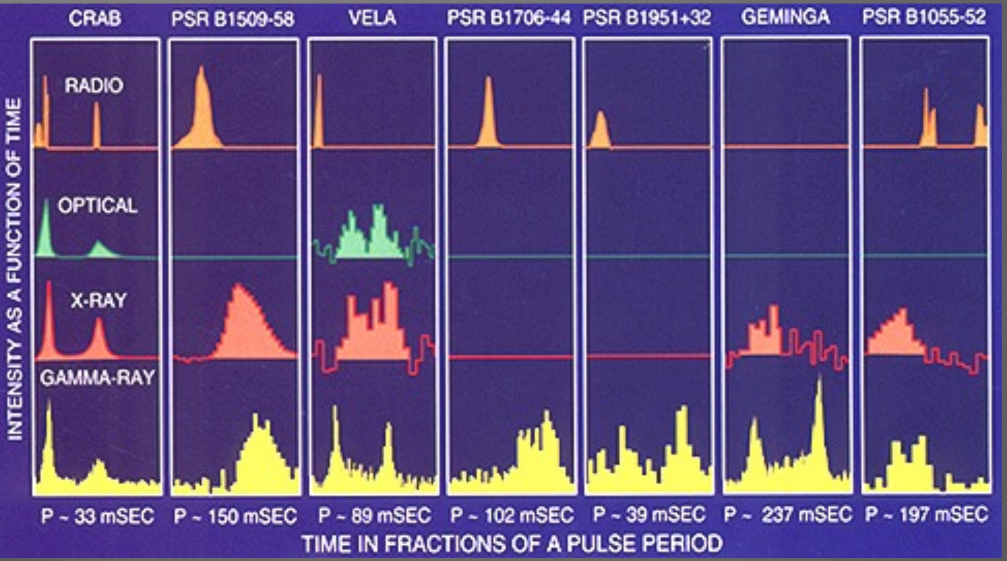

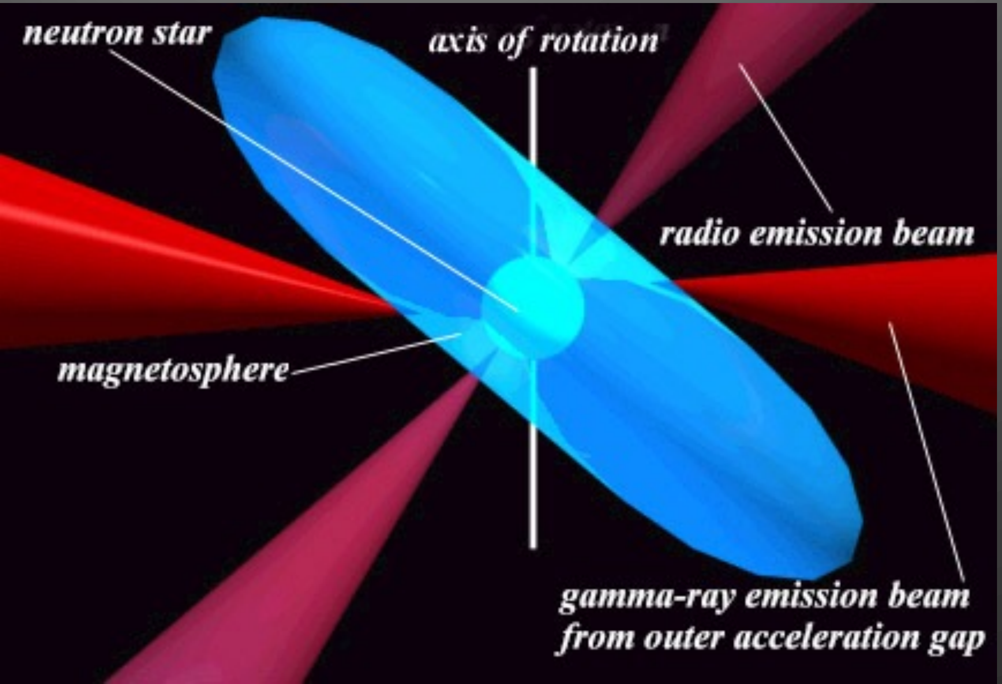

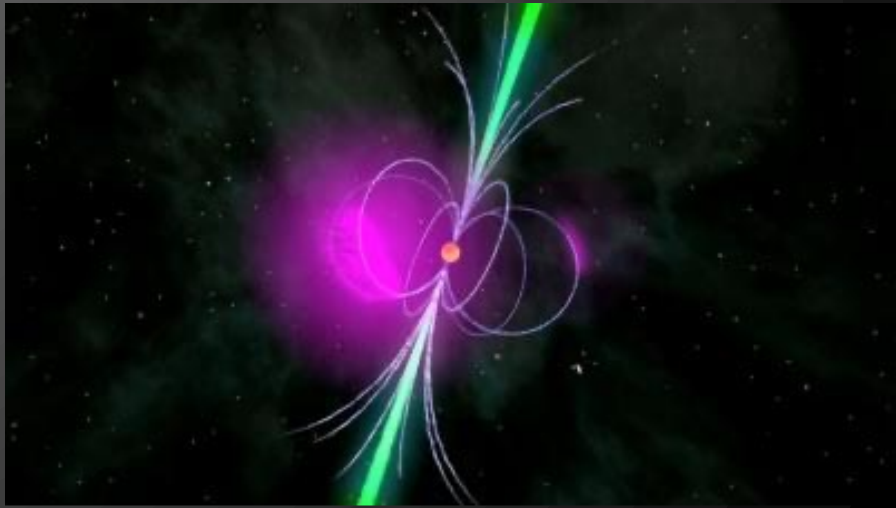

Pulsar pulse profiles

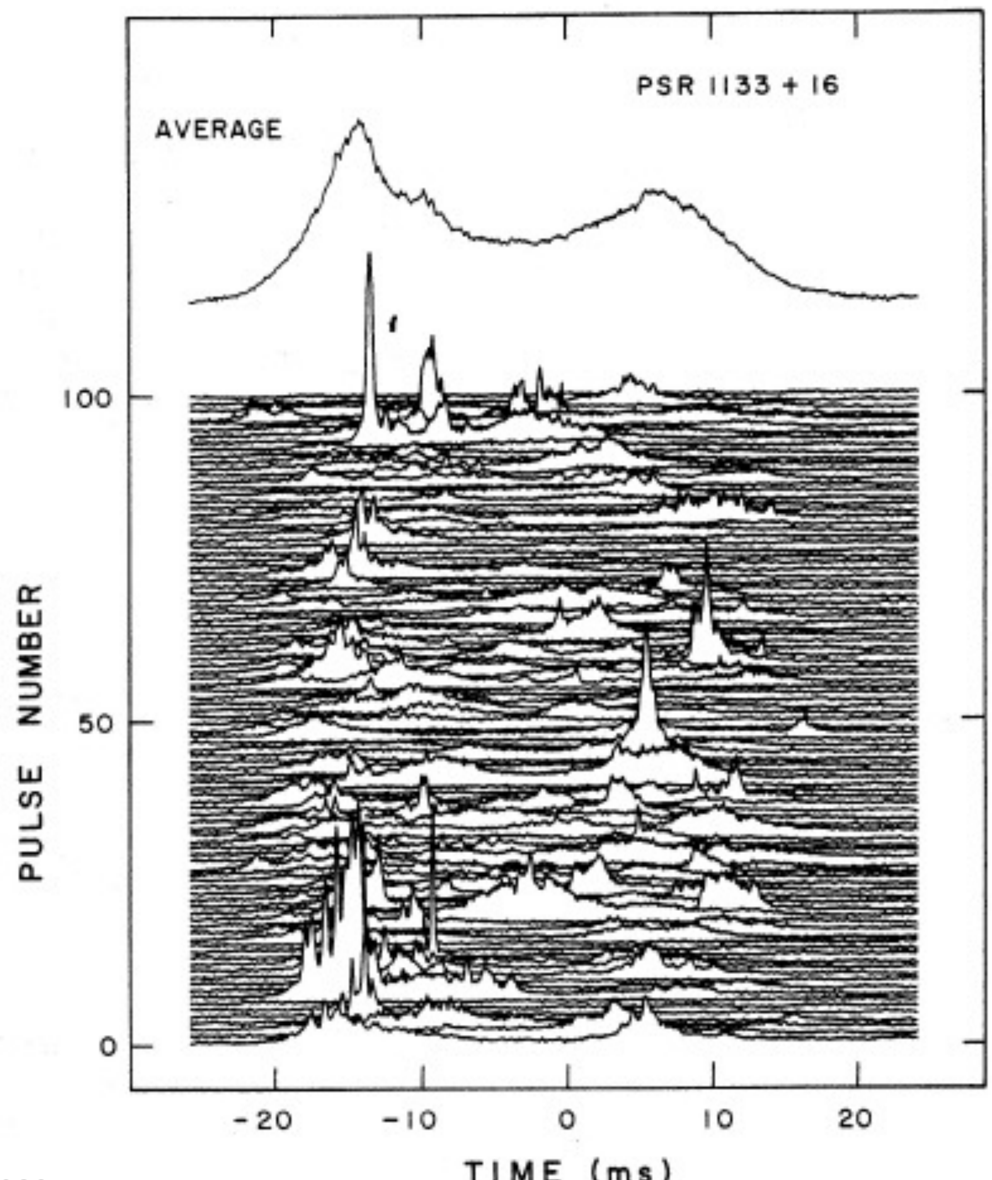

Scintillation (interstellar weather)

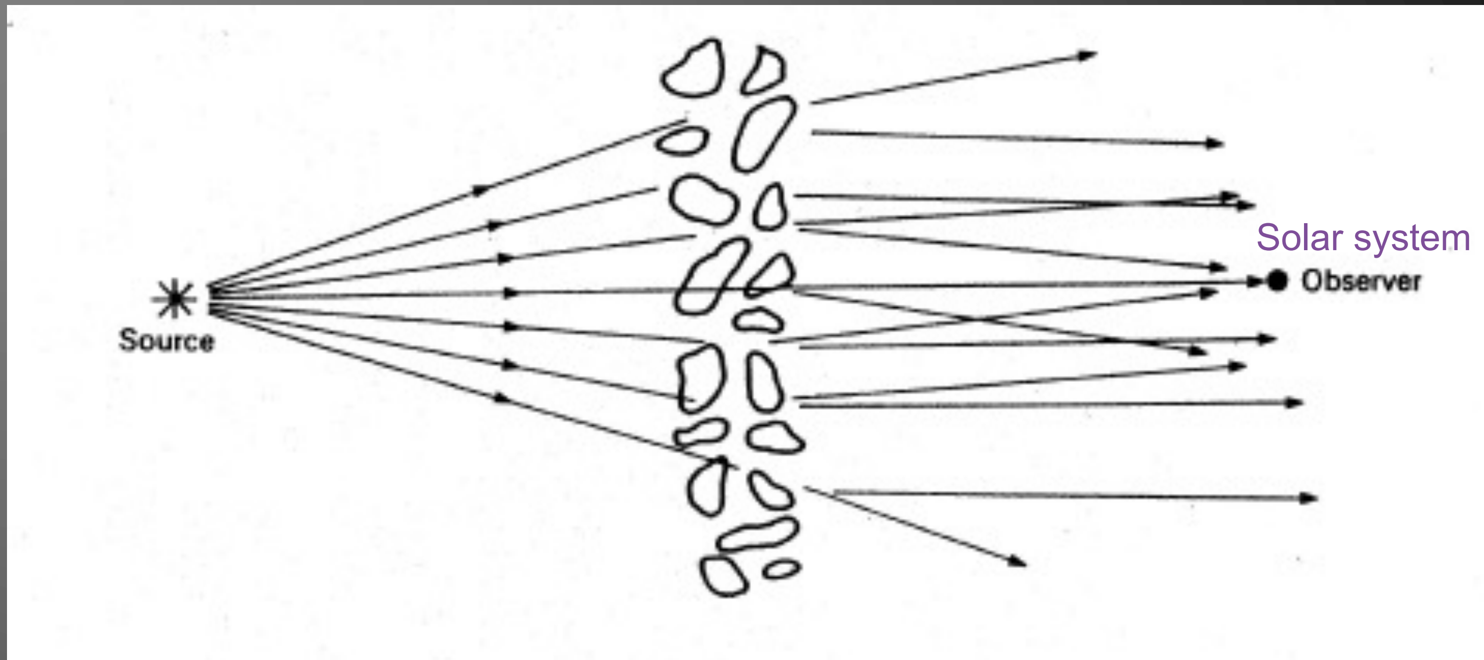

emitted pulse

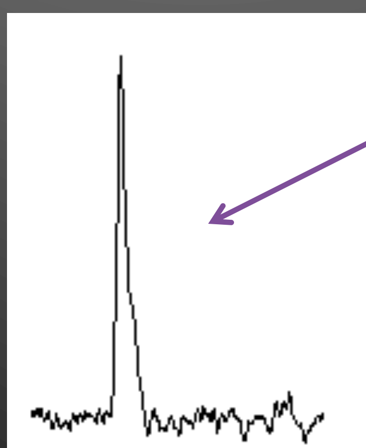

observed pulse

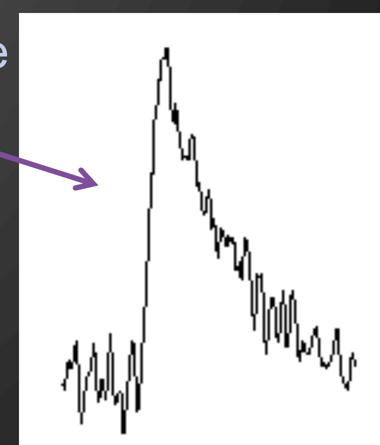

Distance determination of pulsars

452 MHz

256 channels
* 125 kHz

436 MHz
(70 cm)

420 MHz

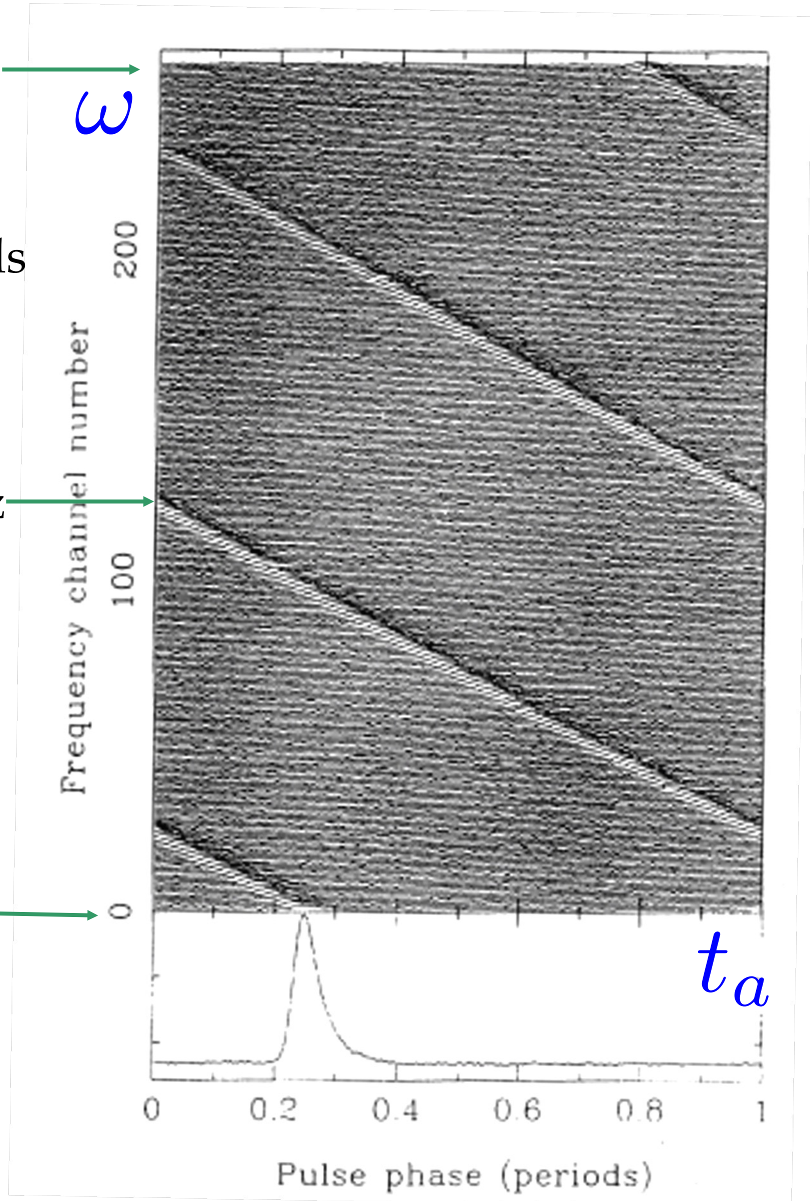

delay in time-of-arrival

dispersion measure

$$\frac{\Delta t_a}{\Delta \omega} = -\frac{4\pi e^2}{m_e c\, \omega^3} DM$$

frequency interval

distance

$$DM = \int_0^L n_e \, dl = \langle n_e \rangle L$$

free electron density

distance (L) α 1/slope

How to find a pulsar ?

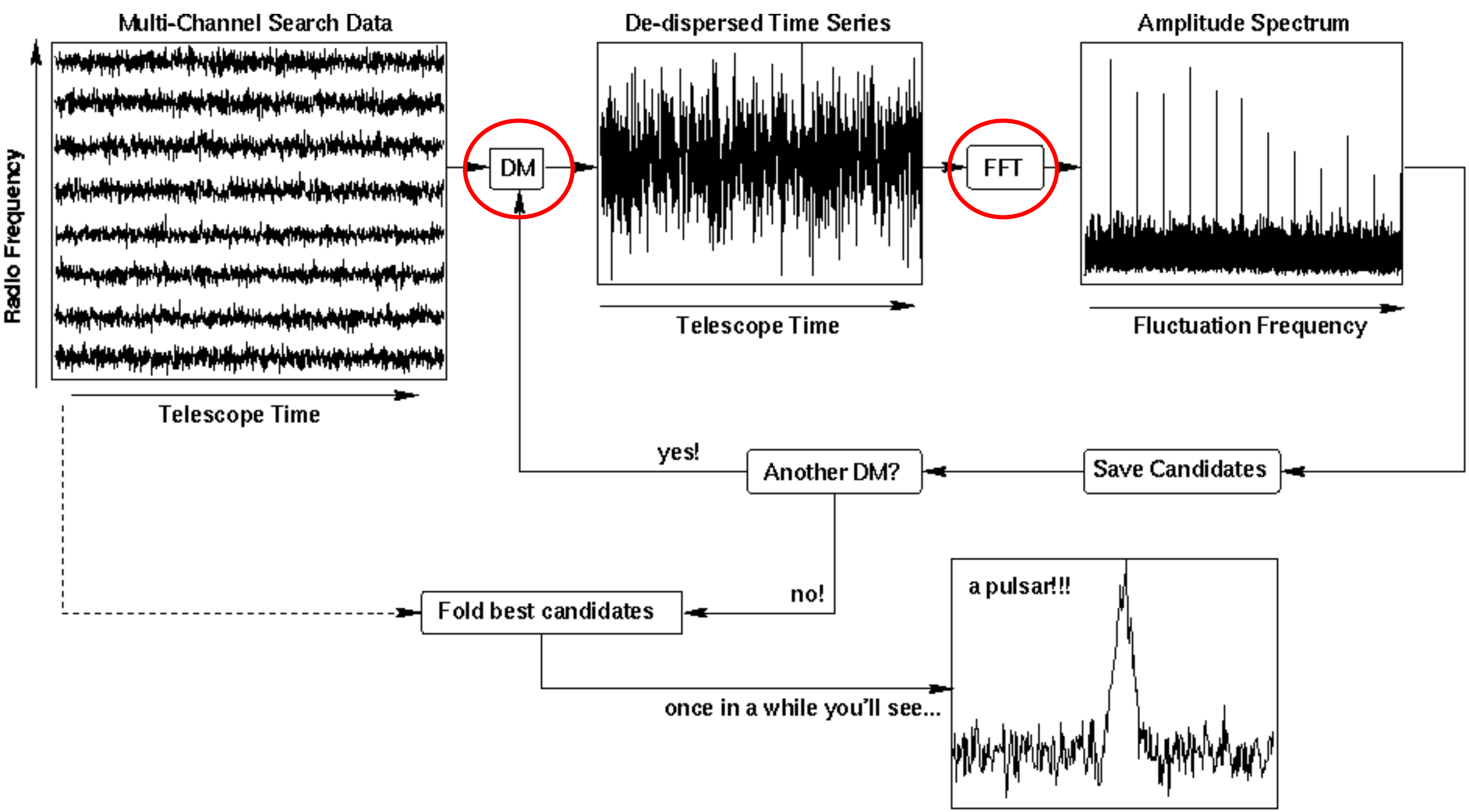

Determination of the stellar wind mass-loss rate of a B-star in the SMC using the measured changes in DM of the binary pulsar PSR J0045-7319

(Kaspi, Tauris & Manchester 1995)

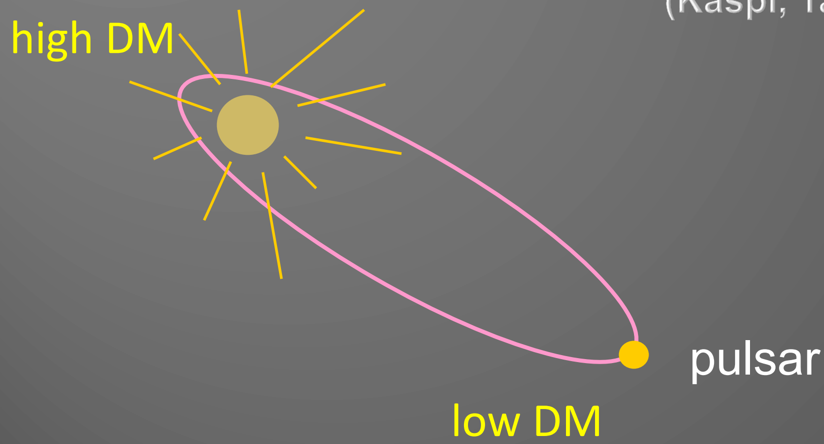

$$\frac{dM}{dt} < 3\times10^{-11}\ M_{\odot}\ yr^{-1}$$

- Most accurate method to determine a stellar wind

Tauris & van den Heuvel (2023)

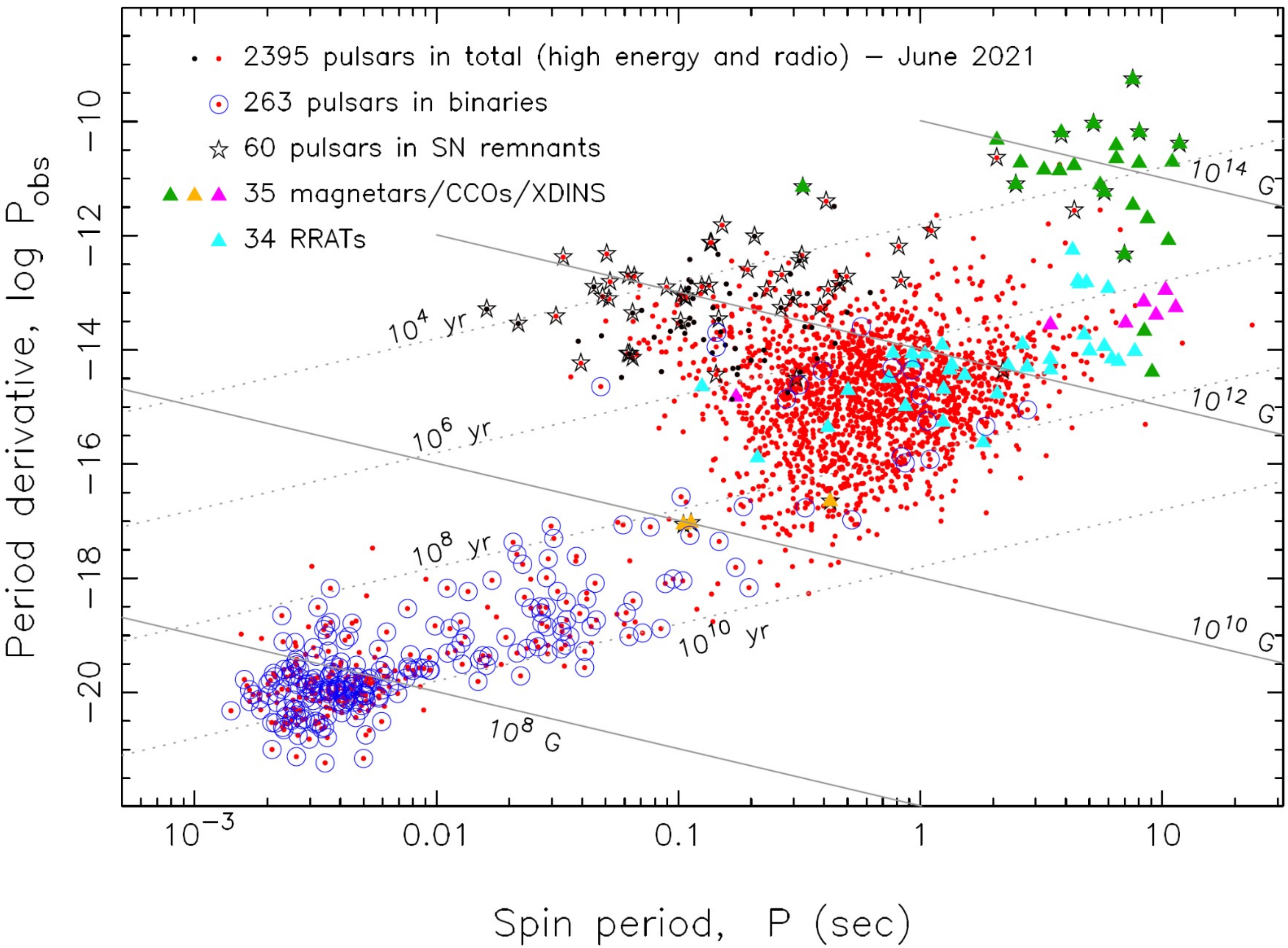

Spin evolution of pulsars

Radio pulsar (P,Ṗ) diagram

The magnetic-dipole model:

$$\dot{E}_{dipole} = -\frac{2}{3c^3}|\ddot{m}|^2$$

second time-derivative of magnetic dipole moment

$$|\ddot{m}| \sim BR^3\Omega^2 \sin\alpha$$

$$E_{rot} = \frac{1}{2} I_{NS}\Omega^2 \quad (\Omega = 2\pi / P)$$

$$\dot{E}_{rot} = I_{NS}\Omega\dot{\Omega}$$

$$\Updownarrow \quad \dot{E}_{rot} = \dot{E}_{dipole}$$

$$\boxed{B = \sqrt{\frac{3c^3 I_{NS}}{8\pi^2 R_{NS}^6} P\dot{P}}}$$

Ex.1

$$\tau \equiv \frac{P}{2\dot{P}}$$ Characteristic age

Active pulsar lifetime: 10-50 million yr

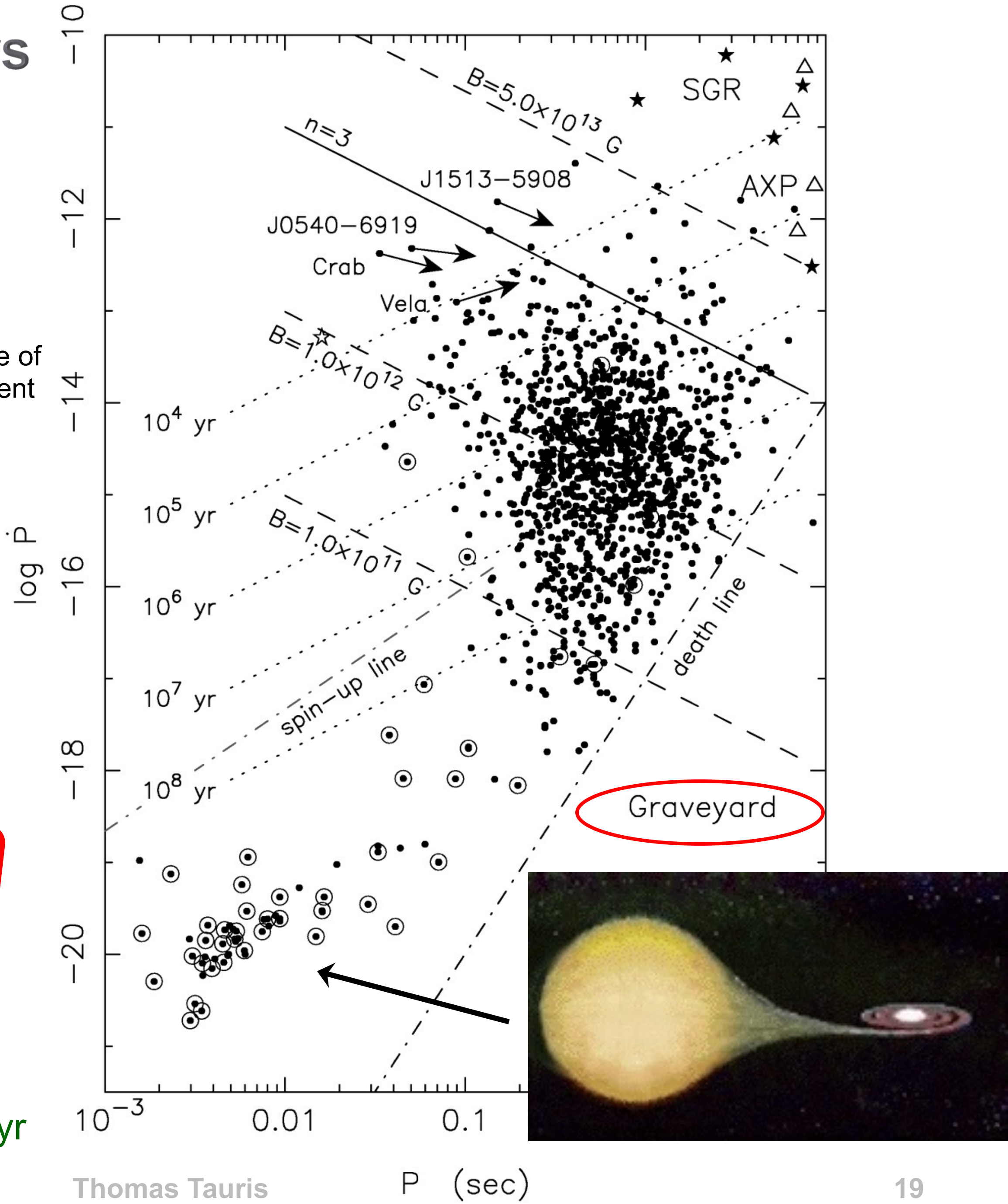

The spin evolution of pulsars

$\dot{\Omega} = -k\,\Omega^n$ the deceleration law, $n = \dfrac{\ddot{\Omega}\Omega}{\dot{\Omega}^2}$ is the braking index

Blackboard

$n = 3$ pure dipole

$n = 5$ pure gravitar (only spin-down by gravitational wave radiation)

Characteristic age

true age of pulsars: $t = \dfrac{P}{(n-1)\dot{P}}\left[1-\left(\dfrac{P_0}{P}\right)^{n-1}\right]$ $\Rightarrow$ $\tau \equiv \dfrac{P}{2\dot{P}}$, for $P \gg P_0,\ n=3$

$$\dot{E}_{dipole} = -\frac{2}{3c^3}|\ddot{m}|^2 \qquad |\ddot{m}| \sim BR^3\Omega^2 \sin\alpha \qquad \dot{E}_{gw} = -\frac{32}{5}\frac{G}{c^5} I^2 \varepsilon^2 \Omega^6$$

second derivative of magnetic moment

$$\dot{E}_{rot} = I\Omega\dot{\Omega} = \dot{E}_{dipole} + \dot{E}_{plasma} + \dot{E}_{gw} \qquad \varepsilon = \frac{a-b}{(a+b)/2}$$

ellipticity (asymmetry $\perp$ rotation axis)

For example:

Ex.3+4

$B(t) = B_0 \cdot e^{-t/\tau_D}$ decay of surface magnetic field

$$P(t)^2 = P_0^2 + B_0^2\,\tau_D\left(1 - e^{-2t/\tau_D}\right)\cdot\frac{1}{k^2} \qquad t \simeq \frac{\tau_D}{2}\ln\left(\frac{2\tau}{\tau_D}+1\right) \qquad \tau \equiv \frac{P}{2\dot{P}}$$

The spin evolution of pulsars

$$\dot{\Omega} = -k\Omega^n \quad \Rightarrow \quad n = \frac{\ddot{\Omega}\Omega}{\dot{\Omega}^2} = 2 - \frac{\ddot{P}P}{\dot{P}^2} \quad \wedge \quad P^{n-2}\dot{P} = const$$

Blackboard

Given $(P_0, \dot{P}_0, n = const, t)$ we can calculate $P(t)$ and $\dot{P}(t)$:

$$P(t) = P_0 \left(1 + (n-1)\frac{\dot{P}_0}{P_0} t \right)^{\frac{1}{n-1}} \qquad \dot{P}(t) = \dot{P}_0 \left(\frac{P(t)}{P_0} \right)^{2-n}$$

(cf. Lazarus et al. (2014) for evolutionary tracks)

$$\boxed{\text{Slope in the } (P, \dot{P}) - \text{diagram:} \quad 2-n}$$

$B = const$: $\dot{P} \propto \frac{1}{P} \quad \Rightarrow \quad -1$ slope

$\tau = const$: $\dot{P} \propto P \quad \Rightarrow \quad +1$

death line: $\Delta\varphi \propto B / P^2 \quad \Leftrightarrow \quad \dot{P} \propto P^3 \quad \Rightarrow \quad +3$

Electrostatic potential across polar caps

spin-up line: $P_{eq} \propto B^{6/7} \quad \Leftrightarrow \quad \dot{P} \propto P^{4/3} \quad \Rightarrow \quad +4/3$

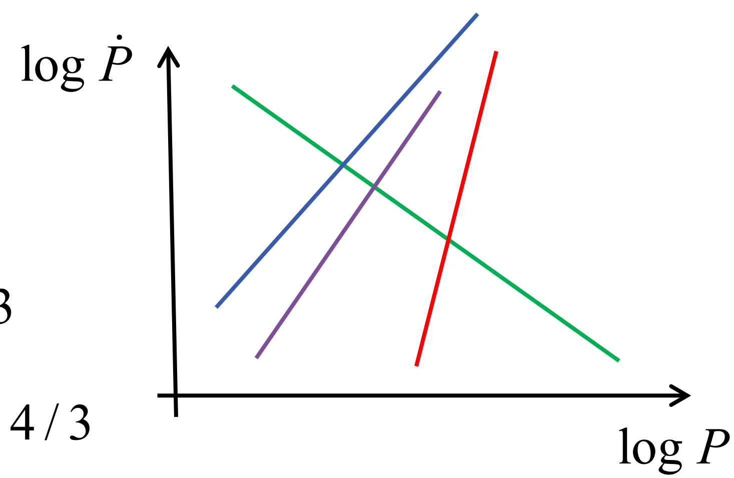

The spin evolution of pulsars

546 T. M. Tauris and S. Konar: Torque decay in the pulsar $(P, \dot{P})$ diagram

Tauris & Konar (2001)

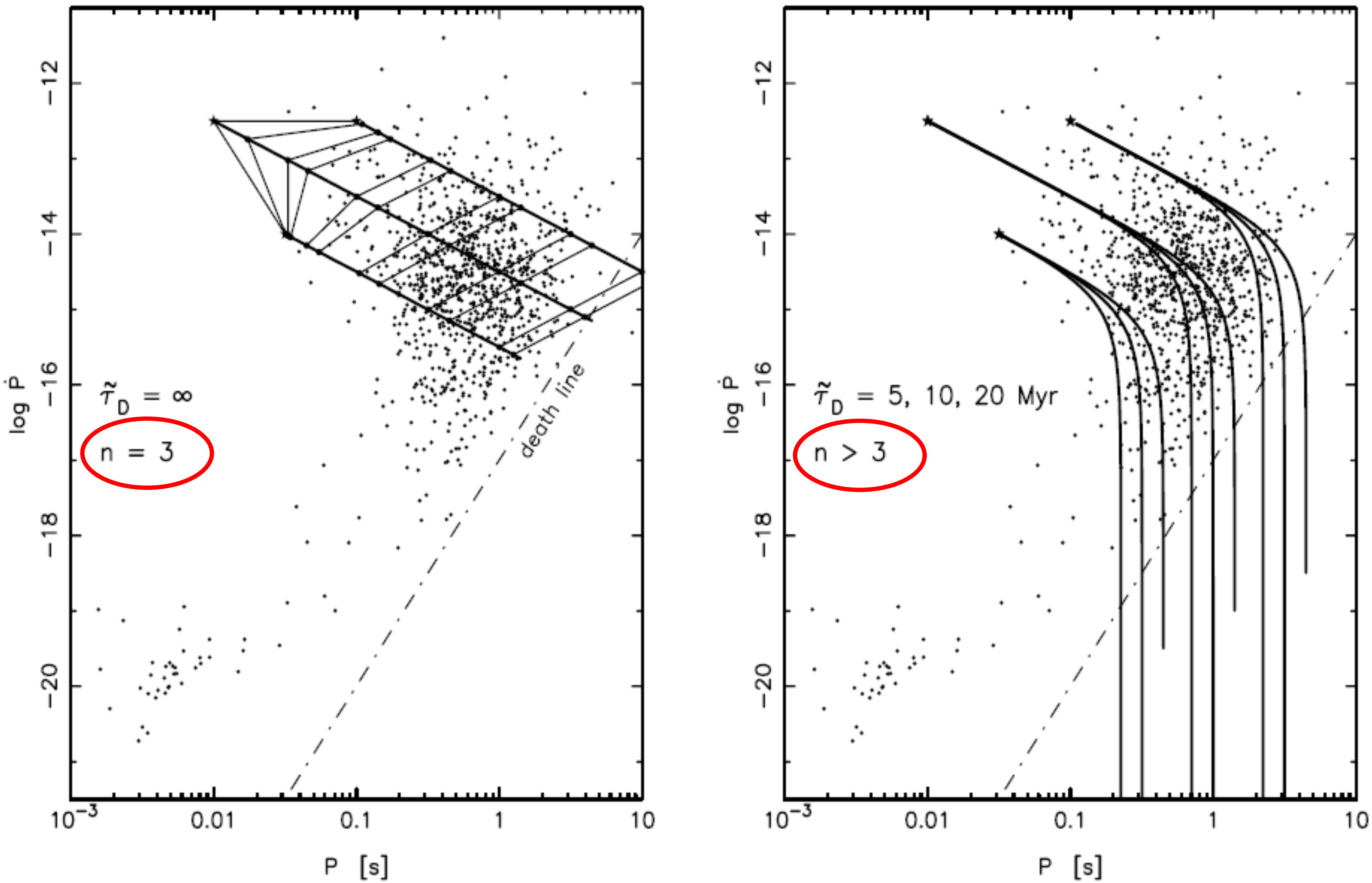

B-field decay in neutron stars, via crustal ohmic dissipation and diffusion, and its dependence on input physics.

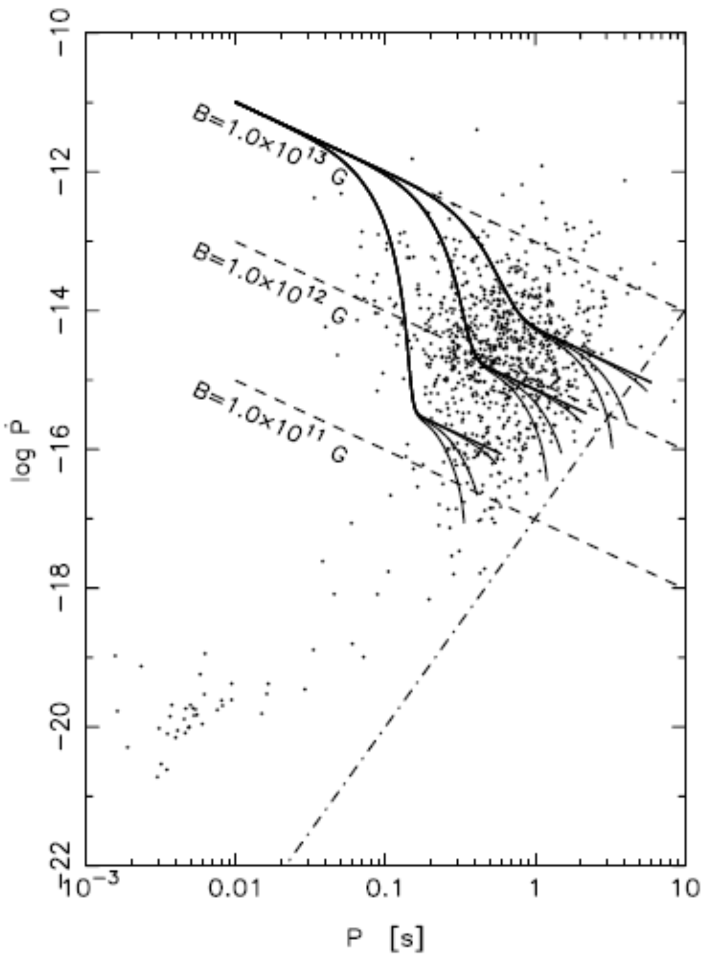

Fig. 6. Evolutionary tracks in the $(P, \dot{P})$ diagram assuming $P_0 = 10$ ms and $\dot{P}_0 = 10^{-11}$ ($B_0 = 10^{13}$ G) calculated from $\rho_0 = 10^{11} - 10^{13}$ g cm^{-3} and $Q = 0$–0.10 – see text. Each track was followed for 100 Myr. The small dots represent data.

$$\boxed{\frac{\partial \vec{B}}{\partial t} = \cancel{\nabla \times \left(\vec{v} \times \vec{B}\right)} - \frac{c^2}{4\pi} \nabla \times \left(\frac{1}{\sigma} \times \nabla \times \vec{B}\right)}$$

$$\boxed{B = \sqrt{\frac{3c^3 I_{NS}}{8\pi^2 R_{NS}^6} P\dot{P}}}$$

A.2. The field evolution equation

We use the form of $B(r, \theta, \phi)$ given by Eq. (A.3) to cast Eq. (A.7) in terms of the Stokes' stream function.

I. The left hand side:

$$\frac{\partial \boldsymbol{B}}{\partial t} = \frac{\partial \nabla \times \boldsymbol{A}}{\partial t} = \nabla \times \frac{\partial}{\partial t}\left[\frac{g(r,\theta)\ \sin\theta}{r}\right] \hat{\phi}. \qquad \text{(A.10)}$$

II. The right hand side:

$$\nabla \times \left[\frac{1}{\sigma} \nabla \times \boldsymbol{B}\right] =$$

$$\nabla \times \left[\frac{1}{\sigma} \nabla \times \left(\frac{2\cos\theta\ g(r,t)}{r^2}\ \hat{r} - \frac{\sin\theta}{r}\ \frac{\partial g(r,t)}{\partial r}\ \hat{\theta}\right)\right] =$$

$$\nabla \times \left[-\frac{1}{\sigma}\ \frac{\sin\theta}{r} \left(\frac{\partial^2 g(r,t)}{\partial r^2} - \frac{2g(r,t)}{r^2}\right) \hat{\phi}\right]. \qquad \text{(A.11)}$$

Incorporation of the expressions (A.10) and (A.11) in Eq. (A.7) then leads to:

$$\frac{\partial g(r,t)}{\partial t} = \frac{c^2}{4\pi\sigma} \left(\frac{\partial^2 g(r,t)}{\partial r^2} - \frac{2g(r,t)}{r^2}\right). \qquad \text{(A.12)}$$

Magnetars

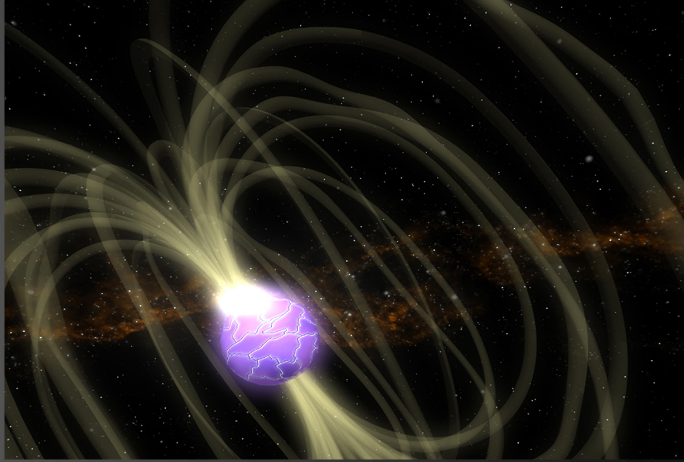

A magnetar is a type of neutron star with an extremely high B-field, the decay of which powers the high-energy emission of anomalous X-ray pulsars (AXPs) and soft gamma-ray repeaters (SGRs).
Duncan & Thompson & (1992) developed the theory to explain these objects.

Support for this extreme B-field picture comes from:

1) Location in P-P_{dot} diagram
2) Cannot be radio pulsars b/c $L_X >> \dot{E}_{rot}$
3) Cannot be X-ray binaries b/c absence of Doppler modulation in timing data
4) Cannot be neutron stars accreting from a fall-back disk b/c of detection of flares
5) Bursts can be explained by magnetic giant flares

Magnetars are detected both as persistent (quiescent) sources and burst sources.

There are currently ~30 known magnetars: 15 SGRs and 15 AXPs according to McGill SGR/AXP online catalogue:

http://www.physics.mcgill.ca/~pulsar/magnetar/main.html

with various burst, transient and persistent properties

Spin Evolution of Magnetars

JOURNAL ARTICLE

Modelling spin evolution of magnetars Get access

Jedrzej A Jawor, Thomas M Tauris

Monthly Notices of the Royal Astronomical Society, Volume 509, Issue 1, January 2022, Pages 634–657, https://doi.org/10.1093/mnras/stab2677

Published: 21 September 2021 **Article history** ▾

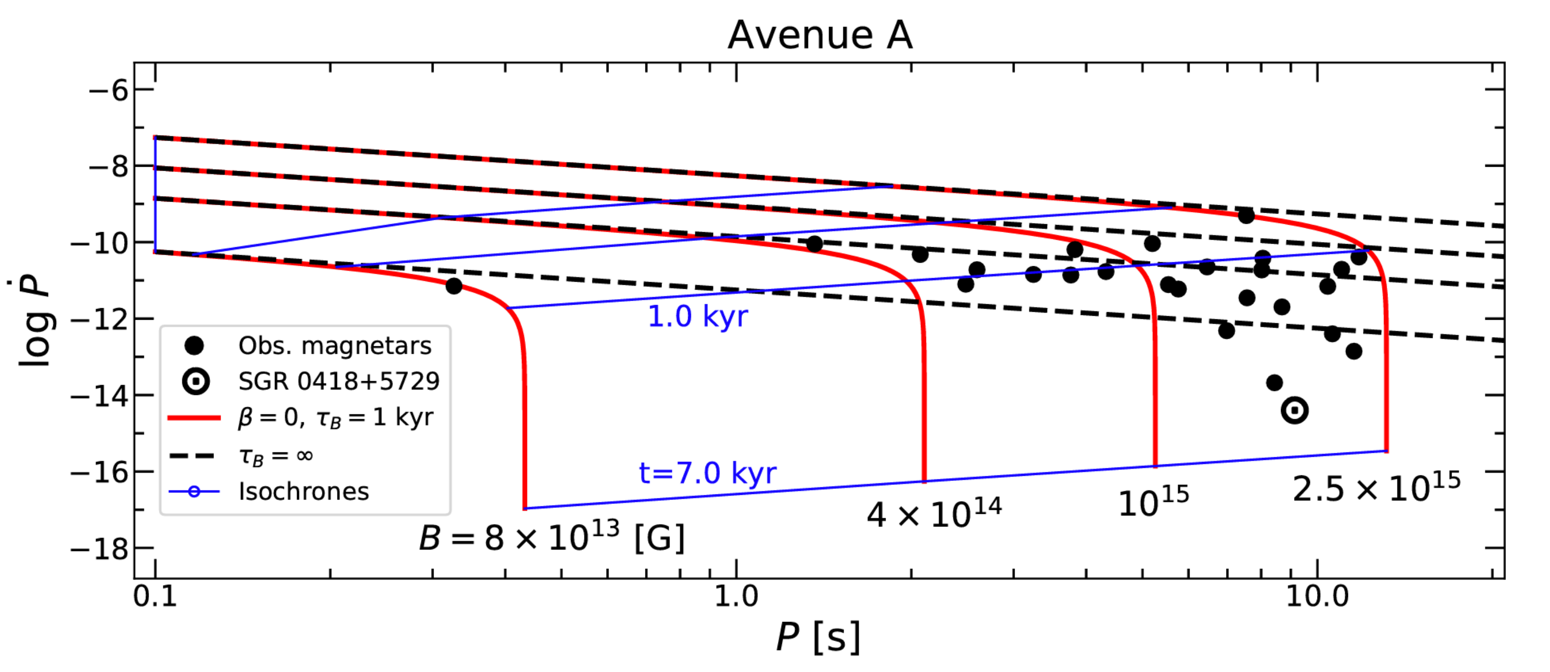

$$P(t) = \begin{cases} \sqrt{\frac{2KB_0^2\,\sin^2\alpha_0\,\tau_B}{\beta-2}\left[\left(1+\frac{\beta\,t}{\tau_B}\right)^{\frac{\beta-2}{\beta}}-1\right]+P_0^2} & \beta \neq 0\,, \\ \sqrt{KB_0^2\,\sin^2\alpha_0\,\tau_B\left(1-\exp\left(\frac{-2t}{\tau_B}\right)\right)+P_0^2} & \beta = 0\,. \end{cases} \quad (12)$$

Jawor & Tauris (2022)

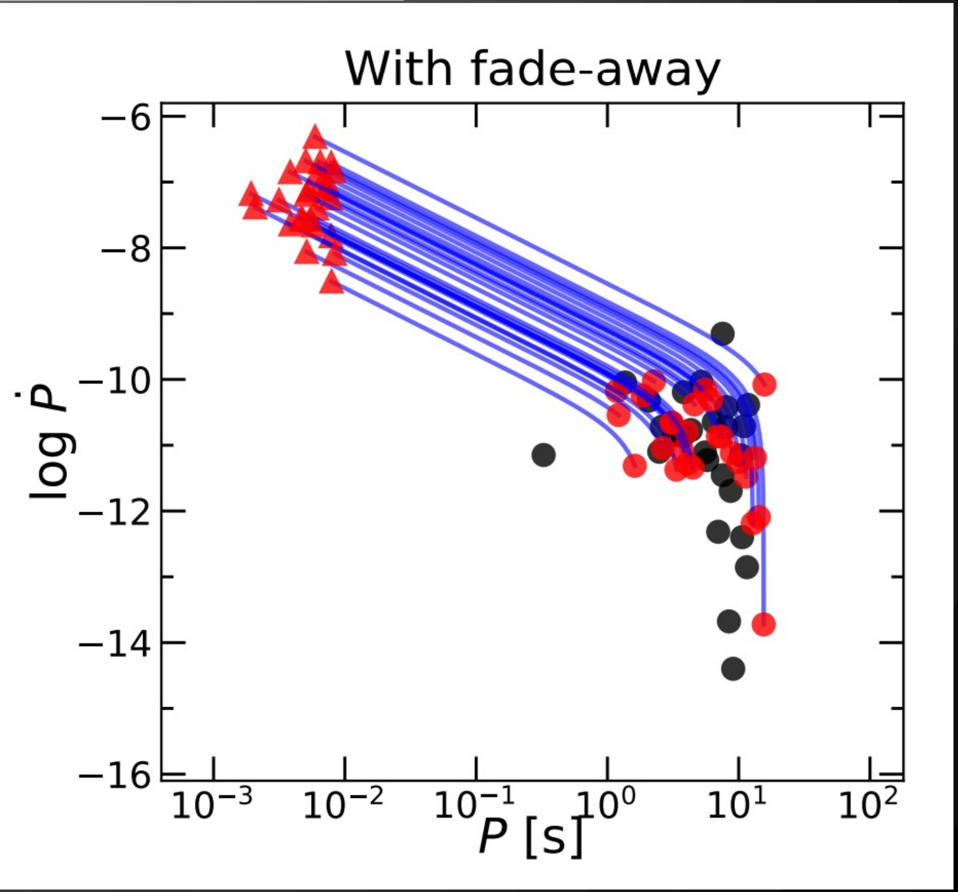

Examples of magnetars (from Silvia Zane)

	Hosts	P (s)	B (10^{14}G)	kT(keV) / Γ	L (10^{33} erg/s) (0.2-10keV)	comments
4U 0142+61		8.7	1.3	0.46 / 3.4	72	hard X
RXS J1708-4009		11	4.7	0.44 / 2.4	80-190	hard X
1E 1841-045	Kes 73	11.8	7.1	0.44 / 2.0	110	hard X
1E 2259+586	CTB 109	7.0	0.6	0.41 / 3.8	17 - 159	~ transient/hard X
CXO J0100-72	in SMC	8.0	3.9	0.38 / 2.0	200	
1E 1048-5937		6.4	3.9	0.63 / 2.9	5.3 - 250	~ transient
1E 1547-5408		2.0	2.2	0.52 / 2.9	2.6 - 170	transient/radio
XTE 1810-197		5.5	2.9	0.67 / 3.7	5 - 260	transient/radio
CXO 1647-4552	in Wes1	10.6	1.5	0.68/2.0	1-130	transient
AX J1845-0258	G29.6+0.1	7.0	-	/ 4.6	5 - 120	transient
SGR 1900+14	OB	5.2	5.7	0.43 / 2.0	200 - 350	GF/hardX
SGR 1806-20	OB	7.5	7.8	0.6 / 1.4	320 - 540	GF/hardX/outburst
SGR 0526-66	in LMC	8.0	7.4	0.53 / 3.1	260	GF/?
SGR 1627-41	G337.0-0.1?	6.4 ?	-	/ 2.9	4 - 100	outburst

Magnetars

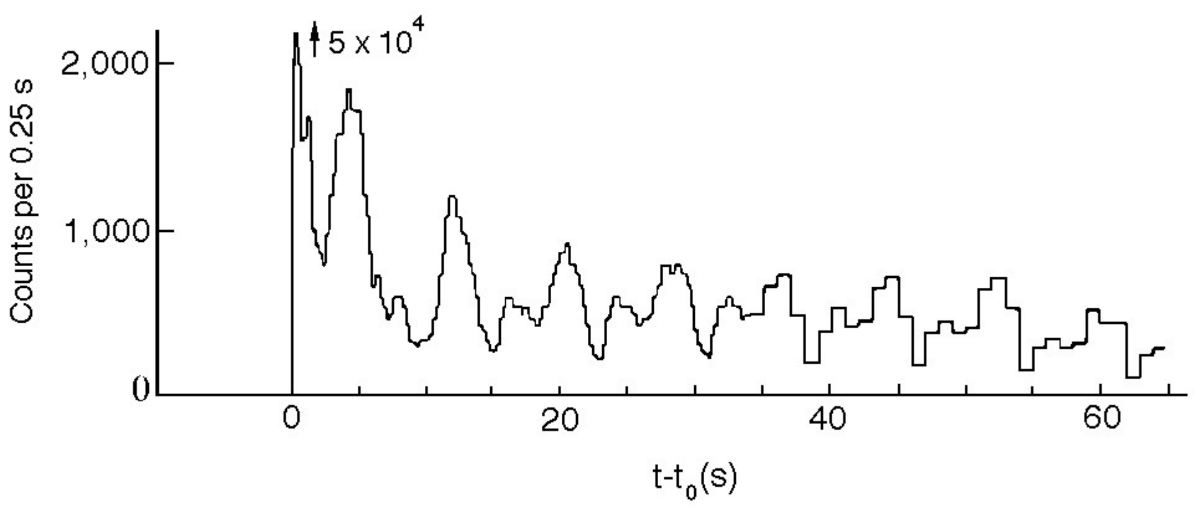

The famous March 5, 1979 event
(the largest burst of gamma-rays ever detected)
Notice, the 8.0 sec cycle (spin period of NS).

16 additional small bursts seen between 1979–1983
and since then no burst have been detected.

The source was located in an LMC SN remnant

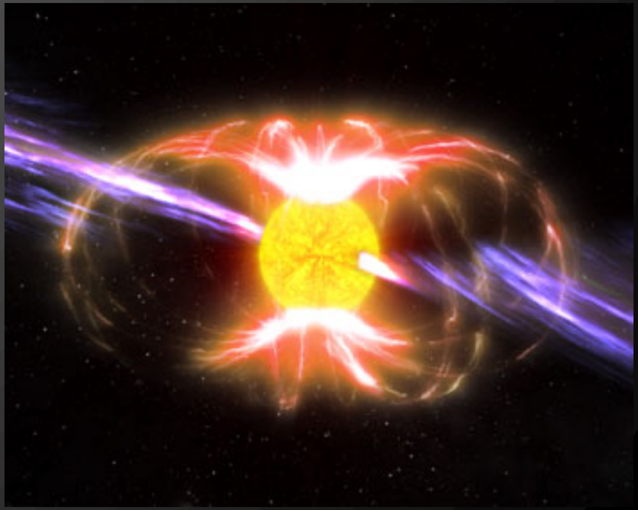

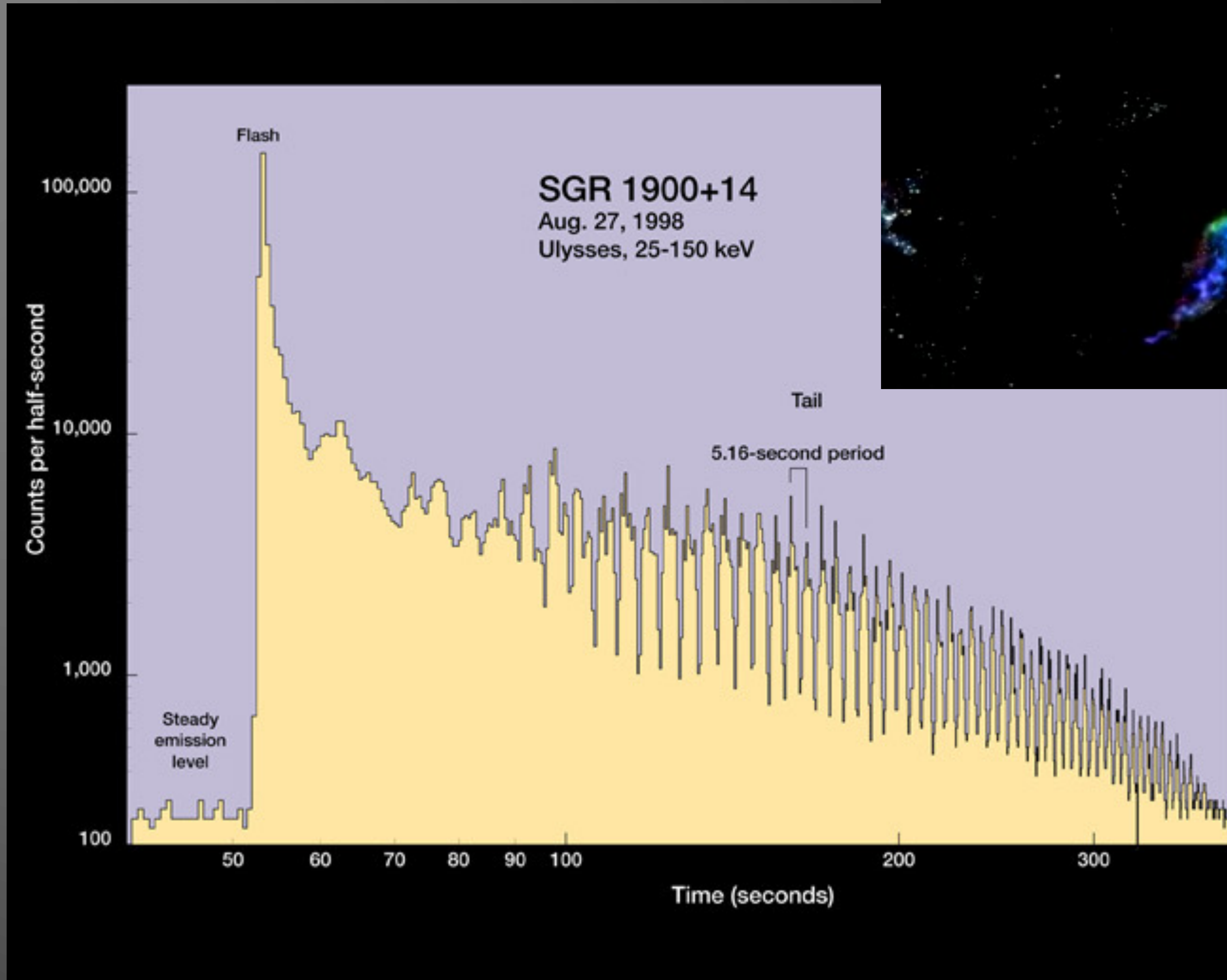

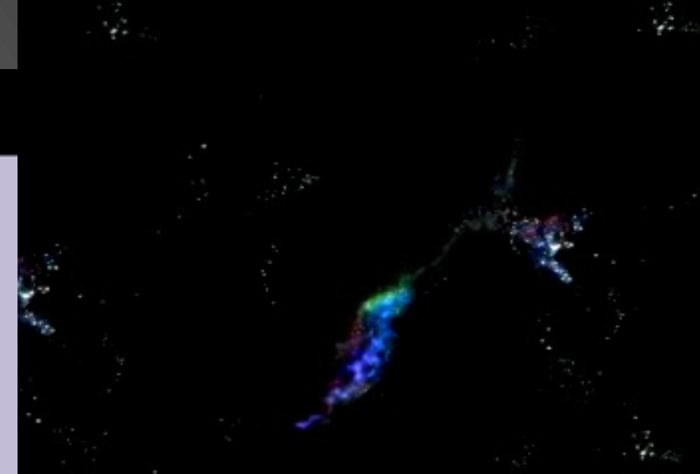

Impact on Earth!

Another famous giant flare (burst) is the August 27, 1998 event (most intense flux of gamma-ray ever detected)

Magnetars

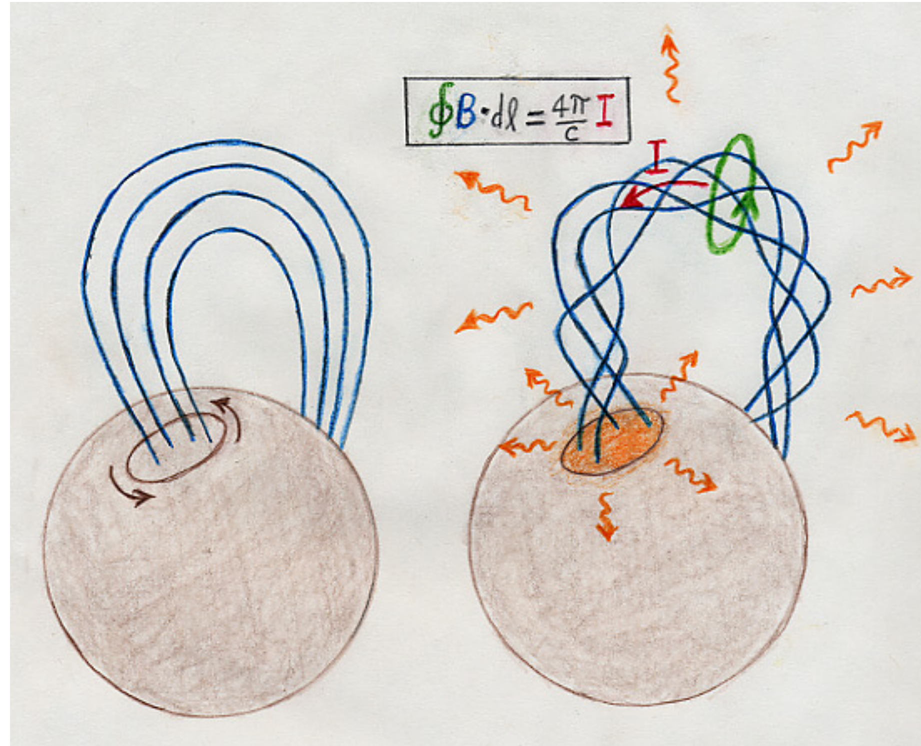

A magnetic twist gives rise to
X-ray emissions from a magnetar.

Robert C. Duncan, University of Texas at Austin

Twisted B-fields support excess currents in the magnetosphere.
Detection of resonant cyclotron scattering reveals the B-field strengths.

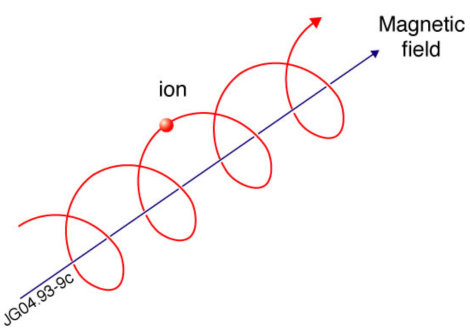

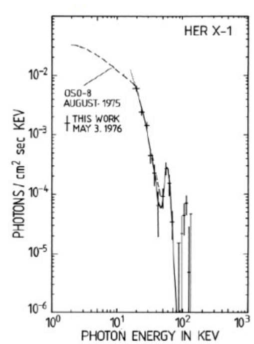

$$E_{cyclotron}^{proton} \approx 0.63 \cdot \sqrt{1 - 2GM / c^2 R} \cdot (B / 10^{14}\, G) \quad \text{keV}$$

Magnetars

Giant flares – a fireball model

Huge tension builds up in the crust from magnetic stress - when released this energy produces a giant flare. A trapped fireball (orange zone) on the surface of a neutron star (brown). The fireball, containing positrons (e^+), electrons (e^-), and high-energy photons (γ), is confined by the magnetic field (dark, arched lines). It loses energy by emitting hard X-ray photons (orange squiggley arrows) from its surface. The fireball also contains a trace of heavy particles (protons and ions) which were blown off the surface of the star. These heavy particles settle down along field lines as the fireball loses energy and shrinks.

Robert C. Duncan, University of Texas at Austin

Magnetars

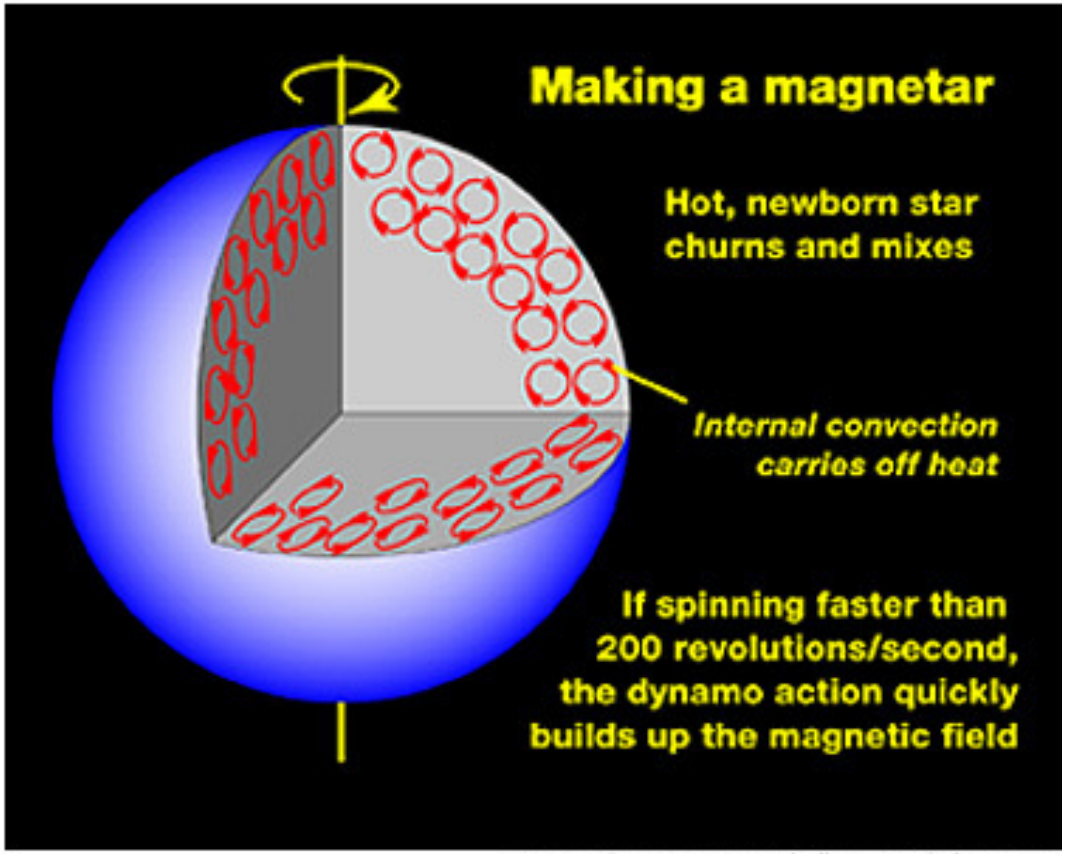

Dave Dooling, NASA Marshall Space Flight Center

Magnetars: AXPs

01 LONG-TERM *RXTE* MONITORING OF 1E 1048.1 – 5937

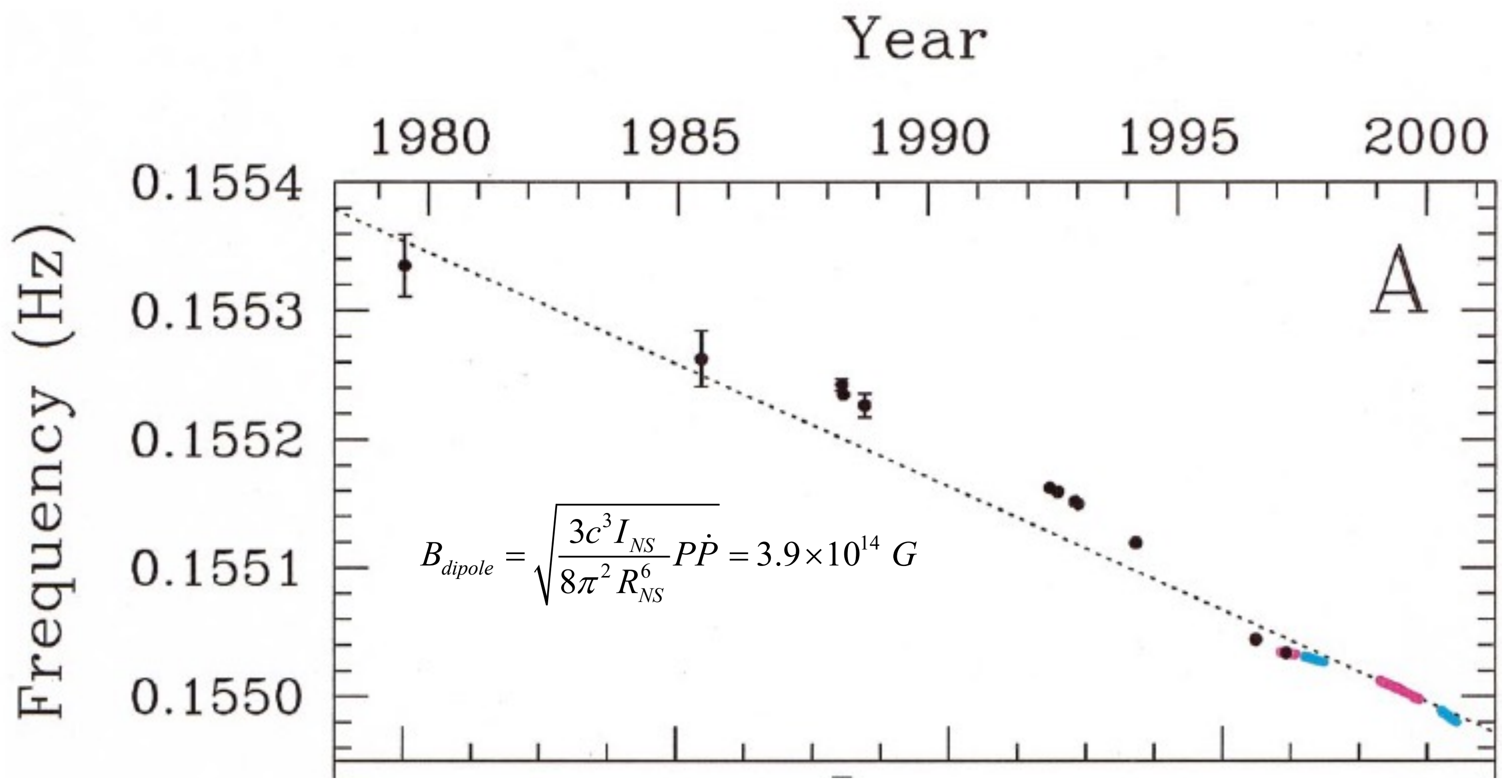

$$B_{dipole} = \sqrt{\frac{3c^3 I_{NS}}{8\pi^2 R_{NS}^6} P\dot{P}} = 3.9 \times 10^{14}\ G$$

Kaspi et al. (2001), ApJ. 558, 253

Grand Unification of Neutron Stars

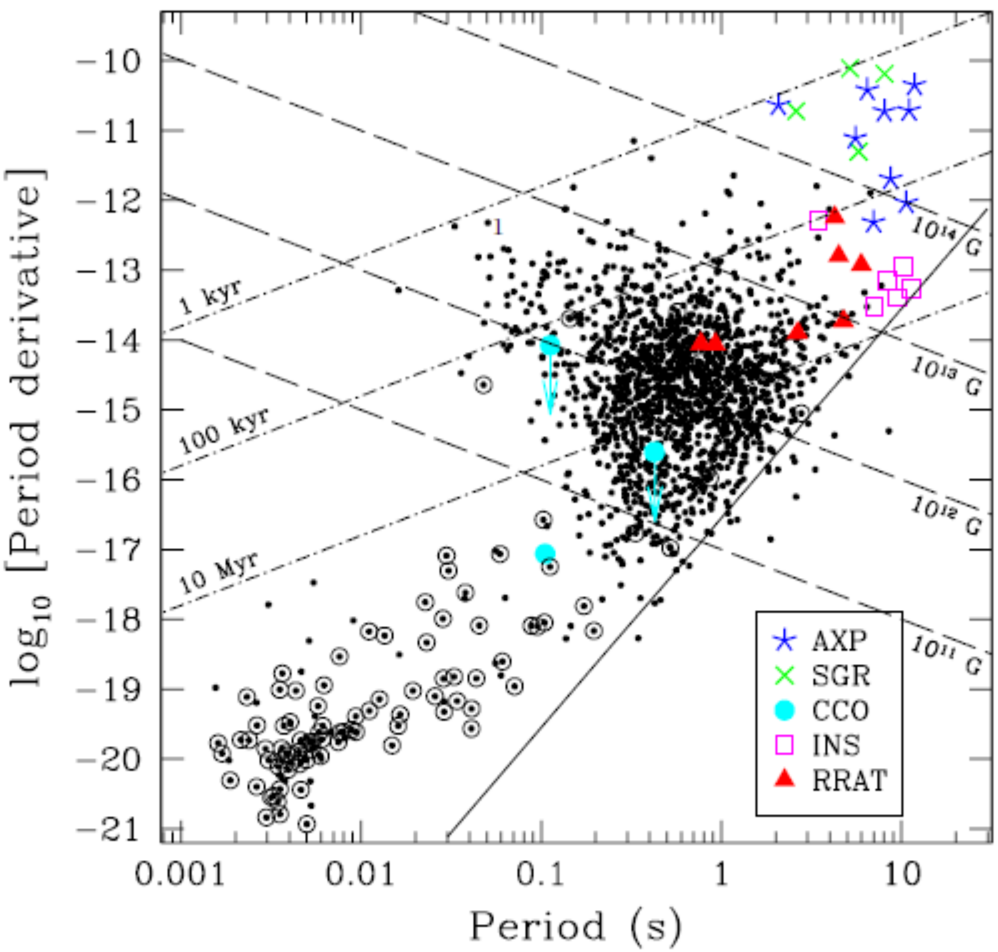

Magnetars are born with rapid spin which creates extremely high B-fields due to convection < 10 sec.

XDINs also have high B-fields.

Radio pulsars are born with moderate B-fields (**RRATs** is a subpopulation).

CCOs (”anti-magnetars”) are born with weak B-fields.

Maybe these neutron star populations are connected with their **evolution** (cf. some radio pulsars have very small brakning indices and evolve *upward* in the PP$_{dot}$-diagram).
Espinoza et al. (2011), ApJ, 741, L13

Summary

Radio Pulsars

Characteristics, observations, spin evolution, magnetars

- Observational aspects of radio pulsars
  - The radio pulsar population in the Milky Way
  - Pulse profiles / Scintillation / Dispersion measure
  - Emission properties
- Spin evolution of pulsars in the $P\dot{P}$-diagram
  - The magnetic dipole model
  - Evolution with B-field decay
  - Evolution with gravitational wave emission
  - The braking index
  - True ages of radio pulsars
- Magnetars
  - Soft gamma-ray repeaters (SGRs) and Anomalous X-ray pulsars (AXPs)

Blackboard

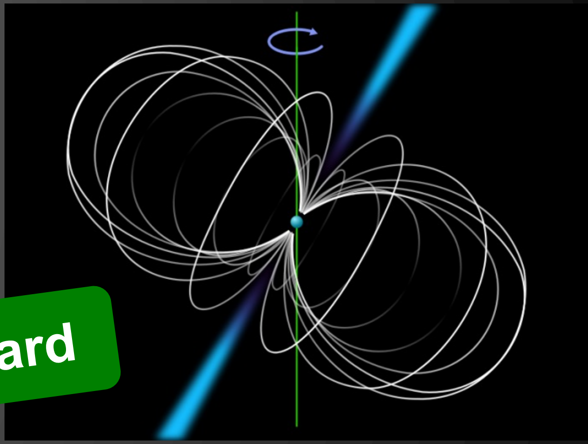

Programme

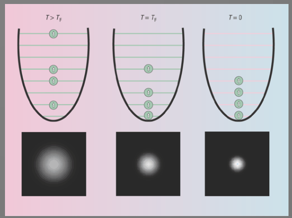

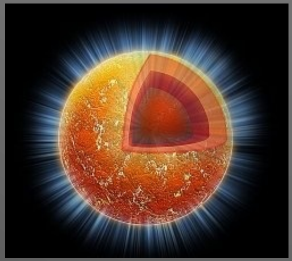

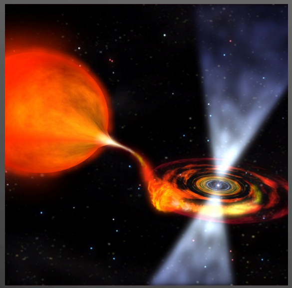

- **Introduction**
- **Degenerate Fermi Gases**
  Non-relativistic and extreme relativistic electron / (n,p,e^-) gases
- **White Dwarfs**
  Structure, cooling models, observations
- **Neutron Stars**
  Structure and equation-of-state
- **Radio Pulsars**
  Characteristics, spin evolution, magnetars, observations
- **Binary Evolution and Interactions**
  X-ray binaries, accretion, formation of millisecond pulsars, recycling
- **Black Holes**
  Observations, characteristics and spins
- **Gravitational Waves**
  Sources and detection, kilonovae
- **Exam**

Physics of Compact Objects
week 6

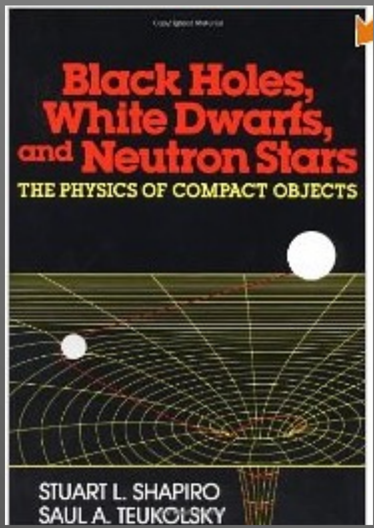

Shapiro & Teukolsky (1983), Wiley-Interscience

Curriculum
- Chapter 10: p.267–290
  + Tauris & van den Heuvel (2023), Chapter 14.1

- Next lecture: Tauris & van den Heuvel (2023), Chapters 4,6,7,10,11 (S&T Chapter 13+15). Aud.2.115.

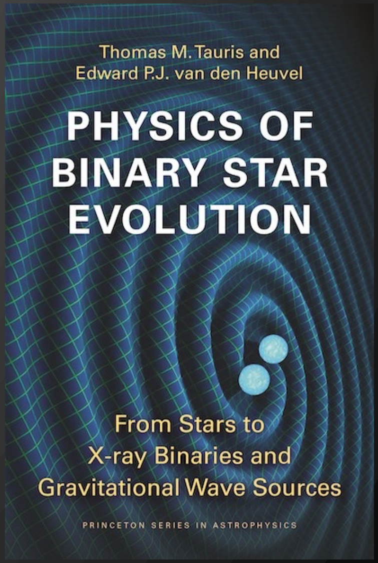

Exercises: # 1−4

- Monday Oct. 9, 10:15-12:00